Soft Matter

ARTICLE

Virus-Like Particles as crosslinkers in fibrous biomimetic hydrogels: Approaches towards capsid rupture and gel repair

Received 00th January 20xx,
Accepted 00th January 20xx

DOI: 10.1039/x0xx00000x

www.rsc.org/

Daniël C. Schoenmakers†,[a], Lise Schoonen†,[a,b], Martin G. T. A. Rutten[a], Roeland J. M. Nolte[a], Alan E. Rowan†,[a,c], Jan C. M. van Hest*,[a,b], Paul H. J. Kouwer*,[a]

Biological hydrogels can become many times stiffer under deformation. This unique ability has only recently been realised in fully synthetic gels. Typically, these networks are composed of semi-flexible polymers and bundles and show such large mechanical responses at very small strains, which makes them particularly suitable for application as strain-responsive materials. In this work, we introduced strain-responsiveness by crosslinking the architecture with a multi-functional virus-like particle. At high stresses, we find that the virus particles disintegrate, which creates an (irreversible) mechanical energy dissipation pathway, analogous to the high stress response of fibrin networks. A cooling-heating cycle allows for re-crosslinking at the damaged site, which gives rise to much stronger hydrogels. Virus particles and capsids are promising drug delivery vehicles and our approach offers an effective strategy to trigger the release mechanically without compromising the mechanical integrity of the host material.

Introduction

Mechano-responsive hydrogels play an important role in nature and are crucial for many cellular processes.[1, 2] These gels are mostly composed of polypeptides and proteins, e.g. collagen, actin and intermediate filaments, which are crosslinked by proteins and/or metal ions. Another interesting example of such a natural gel is fibrin, one of the main structural proteins in blood clots.[3, 4] Upon vascular injury, a fibrin gel is formed, which is one of the most resilient materials known, due to its hierarchical architecture of crosslinked fibers. Although very soft, the fibrin gel is capable of withstanding severe mechanical deformation, because the gel stiffness increases as the stress in the gel increases, an effect called strain or stress-stiffening. A further increase of stress in fibrin cloths result in irreversible disruption of the crosslinkers between the fibers in the network, pulling the hierarchically organised subunits apart whilst the overall architecture of the gel largely remains intact.[5, 6]

Structural biological hydrogels hold great promise for biomedical applications, because of their biocompatibility, mechanical stability, and bioreactivity.[7, 8] Synthetic alternatives to these soft biomaterials that closely mimic the architectural and mechanical properties are relatively rare.[9] They would be very useful as they allow, for instance, the fine-tuning of the gel properties and the introduction of desired functional groups. For biomedical applications, most efforts are currently directed towards the development of crosslinked synthetic or semi-synthetic, which −as a result of their different architecture− lack the characteristic mechanical properties of biological materials.[10-13]

Recently, we reported a fully synthetic hydrogel, which shows an architecture and mechanical properties, including intrinsic strain-stiffening, very similar to biological hydrogels.[14, 15] This dilute gel (<0.5 wt.%) is composed of polyisocyanides (PICs) modified with oligo(ethylene glycol) side chains. The polymers possess a relatively stiff helical backbone and display a lower critical solution temperature (LCST) in water, above which a branched, bundled network is formed. The mechanical properties of the resulting PIC hydrogels can be tuned, e.g. by varying the polymer's molecular weight and concentration,[16] as well as by the conditions, such as the temperature and the ionic strength[17] of the solution. PIC gels combine the architecture and mechanical behaviour of biological gels with the versatility of synthetic gels, making them particularly interesting for biomedical applications, in for instance immunology and regenerative medicine.[18-21]

In contrast to some of the structural biological gels such as fibrin, PIC hydrogels are only marginally able to dissipate stress in its network. After the stiffening response at high strains, the gels simply fracture. Approaches to toughen synthetic, biocompatible hydrogels include the preparation of double network hydrogels,[22-24] bio-synthetic hybrids,[6, 25] and filled nanocomposite gels.[26, 27] In these approaches, however, biomimicry in terms of architecture is often sacrificed for a high polymer density, or the synthetic flexibility is lost by improving the biocompatibility (e.g. by making hybrid gels). In another example, tobacco mosaic virus (TMV) was mixed with alginate

[a] Institute for Molecules and Materials, Radboud University, Heyendaalseweg 135, 6525AJ Nijmegen, The Netherlands.
[b] Eindhoven University of Technology, PO Box 513 (STO 3.31), 5600MB Eindhoven, The Netherlands.
[c] Australian Institute for Bioengineering and Nanotechnology, The University of Queensland, Brisbane, QLD 4072, Australia.
† Both authors contributed equally to this work.

Electronic Supplementary Information (ESI) available: details about VLP expression and functionalization, ESI-TOF analysis results, synthetic procedures and the results of additional rheology experiments. See DOI: 10.1039/x0xx00000x

hydrogels, which improved cell attachment and introduced a non-linear response to compression in these systems.[28, 29] The strategy, however, merely mixed the two components, missing out on the benefits that covalent interaction between the polymers and virus particles bring.

In fact, crosslinking with sacrificial crosslinkers can increase the stiffness of synthetic hydrogels and provide a mechanism for energy dissipation, similar to a fibrin gel. Such approach offers the addition advantage of introducing new functionalities when supramolecular crosslinks are employed.[30] The success of this strategy was recently demonstrated in hydrogels with ionic crosslinks and in gels with crosslinkers of biological origin, such as DNA fragments and or small proteins and peptides.[11, 25, 31-33] The latter have the intrinsic advantage of biocompatibility, making them suitable even for in-vivo applications. Typically, these crosslinkers are bivalent.

To our best of knowledge, the use of a supramolecular protein-based nanocage that can form multivalent sacrificial crosslinks in a hydrogel has not yet been described in the literature. We believe that this type of crosslink not only can stabilise a hydrogel and provide a mechanical energy dissipation mechanism, but can also introduce news function in the material. We envisioned to use protein-based nanocages for this purpose, as they are monodisperse, biocompatible, and robust. The cowpea chlorotic mottle virus (CCMV) capsid, i.e. the empty protein shell of the CCMV virus without the encapsulated endogenous viral RNA, is a particularly interesting protein-based nanoparticle. CCMV is a plant virus with an outer and inner diameter of 28 and 18 nm, respectively.[34] It is composed of 180 identical capsid proteins together forming a icosahedral capsid with a Caspar and Klug triangulation number $T = 3$.[35] This virus is especially interesting, as its capsid proteins are able to reversibly assemble into the $T = 3$ capsids and disassemble back into protein dimers by changing the pH of the buffer solution, even without the viral RNA being present.[36] This pH-sensitive behaviour allows for the creation of highly symmetric and monodisperse particles which can be used as nano-sized carriers for functional cargoes, such as catalysts or enzymes.[37, 38] CCMV capsids have also proved to be useful for applications in materials science, e.g. as components of metamaterials.[39, 40]

Here, we report on the mechanical consequences of covalently crosslinking semi-flexible hydrogels with virus-like particles, which act as multi-functional sacrificial supramolecular crosslink nodes. We covalently attached CCMV capsids to the PIC-based hydrogels through click chemistry techniques (Figure 1). In the composite, we find fibrin-like energy dissipation process that we attribute to stress-induced rupture of the crosslinkers, but a cooling cycle allows the material to heal the

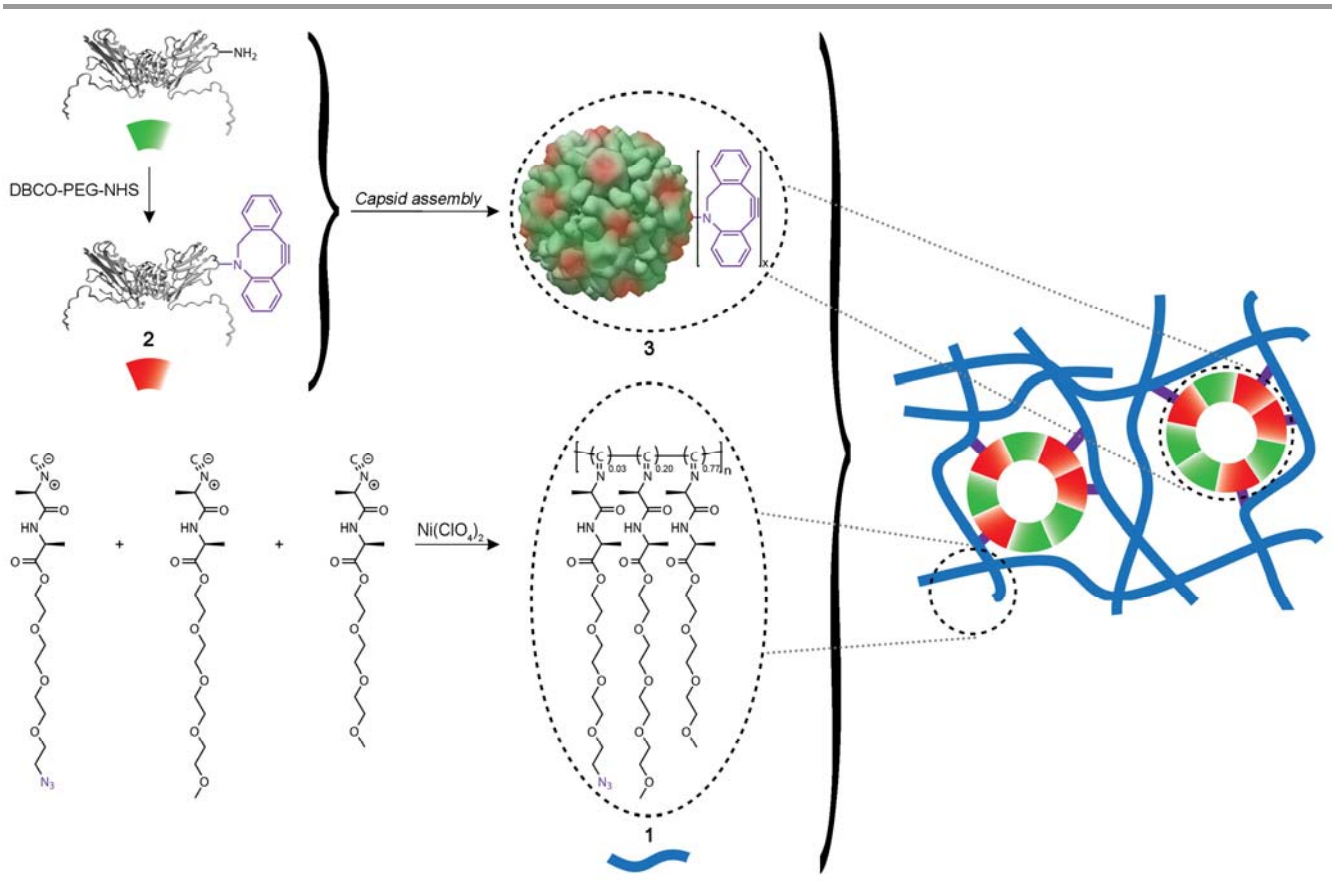

Figure 1. Schematic overview showing the crosslinking of an azide-functionalised polyisocyanide (PIC) hydrogel with DBCO-functionalised cowpea chlorotic mottle virus (CCMV) capsids. The PIC polymers **1** contain 3 % azide-functionalised monomers, 20 % tetra(ethylene glycol) monomers, and 77 % tri(ethylene glycol) monomers. The empty CCMV capsids **3** are assembled (pH change) from a mixture of capsid protein dimers with (red wedge, **2**) and without (green wedge) attached DBCO-groups.

damaged sites. Additionally, we can tune the modulus of the crosslinked gel by changing the degree of functionalisation of the particles, as well as the density of particles in the polymer gel. This crosslinked hydrogel could be very promising for application in mechanical strain-activated functional materials, such as stress sensors or localised drug delivery systems.

Results and discussion

Material synthesis and characterisation

To form a covalent link between the PIC polymers and the CCMV capsid nodes, we used a strategy based on strain-promoted alkyne-azide cycloaddition (SPAAC) click chemistry. Its high efficiency and the lack of an additional catalyst allows us to carry out the crosslinking reaction in the gel state at high dilution.[41] In addition, our groups earlier developed the necessary building blocks.[42, 43] Crosslinkable polymers were acquired by co-polymerizing approximately 3% azide-functionalised monomers. To obtain PIC copolymers with an LCST between 10 °C and 20 °C in the physiological buffer solutions (required for the virus particles[17, 41]), we added a small amount of tetra(ethylene glycol) functionalised monomer to the polymerisation mixture (Figure 1).[44] Random copolymerisation using nickel perchlorate as a catalyst followed standard procedures.[20] After purification by multiple precipitations, the polymer length was determined by viscometry and yielding M_v = 486 kDa and 585 kDa for two independently polymerised batches. Hydrogels were formed by dissolving the polymers in cold buffer solution (0.2 wt.%, see Supporting Information) and heating them beyond the LCST = 12 °C. The mechanical properties of the hydrogels and crosslinked hydrogels were studied by rheology (see Supporting Information for experimental procedures and characterisation). Attempts to characterise the network by (cryo)electron microscopy techniques persistently gave collapsed networks.

CCMV capsids were equipped with dibenzocyclooctyne (DBCO) groups, the complementary group for the SPAAC reaction. To this end, recombinant CCMV capsid proteins were expressed in *Escherichia coli* (*E. coli*), followed by purification through Ni^{2+} affinity chromatography (see Supporting Information for experimental procedures and characterisation). Subsequently, the lysines of the capsid protein dimers were aspecifically modified with dibenzocyclooctyne-PEG_4-*N*-hydroxysuccinimidyl ester (DBCO-PEG4-NHS) molecules, such that a mixture of non-, mono- and bis-DBCO-functionalised capsid protein monomers was obtained (Figure 1 and Supporting Information).[45] Considering that the capsid proteins are always present as dimers in a neutral environment, the functionalisation reaction yielded a statistical mixture of dimers **2** with 0-4 DBCO groups per dimer. At decreased pH, the modified capsid protein dimers **2** successfully assembled into capsids **3** as indicated by size-exclusion chromatography (SEC) analysis. The available DBCO groups on the exterior of the capsid are available for the click reaction with the azide-functionalised polymer **1**. One should realise that because of the aspecific nature of the NHS reaction, of all introduced DBCO-groups (on average approximately 90 per particle) a fraction will be unavailable for crosslinking, as they may be located in the capsid interior of in the protein coat.

Mechanical properties at small deformations

Rheology experiments were carried out to evaluate the mechanical properties of the CCMV-crosslinked and the non-crosslinked hydrogels. For the crosslinking experiments, a pre-cooled solution of either CCMV-DBCO dimers **2** (in buffer at pH 7.5) or capsids **3** (at pH 5.0) was mixed with a cold solution of PIC-N_3 **1** in the same buffer (Figure 2A). Both the DBCO-functionalised capsids **3** and CCMV protein dimers **2** should be able to act as crosslinkers in the PIC network. The dimer-crosslinked PIC network was included in our study, as a suitable model system of a capsid-crosslinked network in which the supramolecular CCMV capsids are ruptured due to high stresses, *vide infra*. The low concentration of crosslink nodes (< 100 μM), prevented us from quantitatively following the crosslinking reaction, but earlier work showed that this reaction at comparable conditions proceeds fast and in excellent yields, even when large (biological) molecules are conjugated.[46] Also, the multi-valency of the crosslinker allows for the formation of a crosslinked networks, even if full conversion of the click reaction is not achieved.

After combining the pre-cooled polymer and the crosslinker solutions, the mixture was transferred to the rheometer, which was immediately heated to 25 °C to induce gelation. As the click-reaction was allowed to proceed for one hour at this temperature, above the LCST of the polymers, the storage modulus G' was measured (Figure 2B). Both samples containing CCMV (dimers: red line and capsids; orange line) and the control samples without the crosslinker (dimer buffer; green line and capsid buffer; blue line) clearly formed elastic gels at 25 °C. The presence of the crosslinker has a negligible effect on the storage moduli at temperatures above the LCST. After cooling to 5 °C, the control samples without crosslinker present turned into viscous solutions (Figure 2C) with minimal moduli and high phase angles ($\tan \delta \approx 0.95$). The crosslinked samples remained a gel ($\tan \delta < 0.2$), albeit relatively weak; the storage modulus of the dimer-crosslinked gel was approximately ten times higher than that of the capsid-crosslinked gel. To estimate the crosslink density in the resulting gels, we compared the values of G' to values obtain in earlier work, which were obtained using a bivalent crosslinker.[41] With the comment that the functionality of the crosslinks in both systems is rather different, we estimate the crosslink density to be approximately 8 μM and 25 μM for capsid and dimers crosslinks, respectively. This difference is explained by the fact that at the same protein concentration, the effective crosslinker concentration in the dimer-crosslinked gel is much higher than in the capsid-crosslinked gel, as in each virus capsid 90 dimers are concentrated. Additionally, not each dimer can act as a crosslinker, as some dimers have less than two DBCO groups attached.

Next, the samples were heated to T = 37 °C to induce the formation of a stiffer gel (PIC gels increase in stiffness with temperature due to the increasing persistence length of the

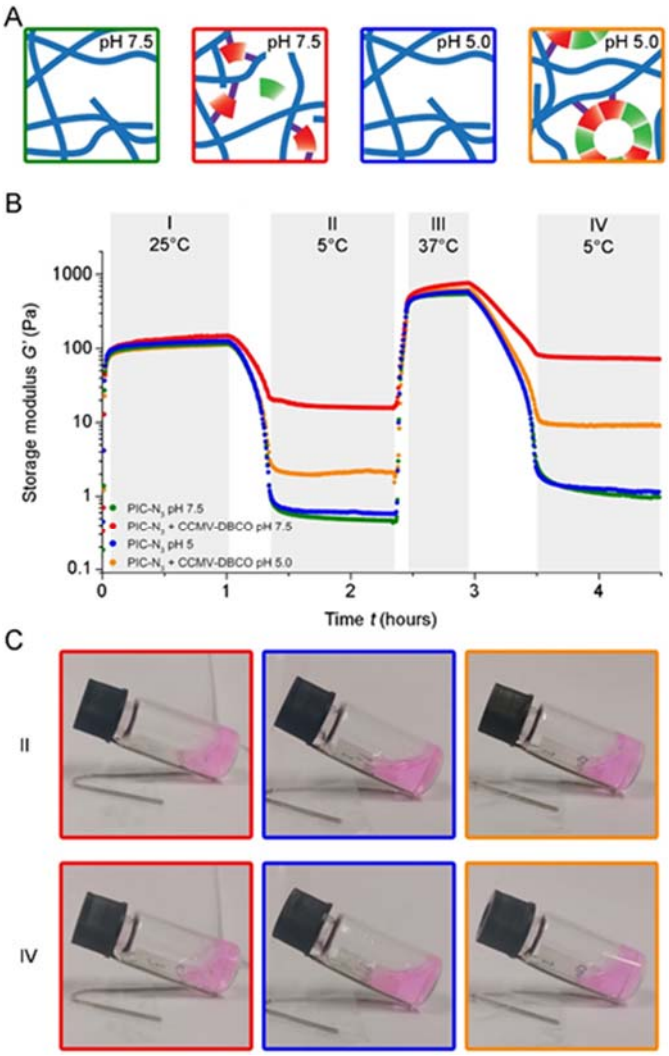

Figure 2. (A) Schematic representation of the four types of PIC gels that were analysed using rheology. Green: polymer **1** in pH 7.5 buffer; Red: polymer **1** + CCMV-DBCO capsid protein dimers **2** in pH 7.5 buffer; Blue: polymer **1** in pH 5.0 buffer; Orange: polymer **1** + CCMV-DBCO capsids **3** in pH 5.0 buffer. (B) Hydrogel storage modulus G' of the PIC gels depicted in Figure A at [**1**] = 2 mg mL^{-1} as measured in the linear viscoelastic regime (γ = 4 % and σ < 10 Pa). The modulus is plotted as a function of the time. Over time, the temperature of the samples was changed as indicated in the graph. The colour coding of the curves corresponds to the situation depicted in Figure A. (C) Dimer- (red) and capsid-crosslinked (orange) PIC hydrogels, and the non-crosslinked PIC solution at pH 5.0 (blue) at 5 °C (II and IV coincide with the temperature zones in B). For visualization, the gels were stained with 6.7 μM Rhodamine B.

polymer chains[15]) and consequently to a stiffer crosslinked network at temperatures below the LCST.[41] At elevated temperatures, all samples mechanically behave identical again. After cooling back to 5 °C, the difference between the crosslinked samples and the controls became even more apparent. While both non-crosslinked controls returned to a viscous liquid, storage moduli of soft gels were obtained for the gel with capsid crosslinks **3** (G' = 9 Pa) and with dimer crosslinks **2** (G' = 80 Pa).

The higher stiffness of the dimer-crosslinked gel is the result of the higher crosslinker density. To further investigate the effect of crosslinker concentration, we performed two more experiments for which we prepared three batches of capsids with different degrees of DBCO-functionalisation, which was controlled by varying the time that the functionalisation reaction was allowed to proceed (Figure S1). In the first experiment, the DBCO concentration was kept constant, but was distributed over fewer capsids, i.e. the DBCO density per capsid increased (schematically depicted below Figure 3A). Note that non-functional capsids were added to keep the total capsid concentration constant over the experiment. After the abovementioned heating and cooling protocol (25→5→37→5 °C), we similarly estimated the crosslink density, referenced to our earlier work (Figure 3A). When DBCO is distributed over more capsids (i.e. at lower DBCO concentration per capsid), the gels show a higher modulus, indicative of a higher crosslinking density. When the density of capsids was kept constant, but the DBCO density per capsid was changed (Figure 3B), modulus and crosslink density variations were insignificant. The results confirm that in our multi-functional CCMV capsid crosslinker, it is the capsid density and not the degree of DBCO-functionalisation of the capsid that limits the crosslinking density and with that, the mechanical properties of the gel at low temperatures.

Mechanical properties at large deformations

Due to the bundled, semi-flexible architecture of PIC hydrogels, they show intrinsic strain-stiffening behaviour at low stresses, i.e. they reversibly stiffen upon deformation beyond a critical value.[2, 47] This stress-response is uncommon in synthetic gels, but many hydrogels of structural biopolymers, such as actin,

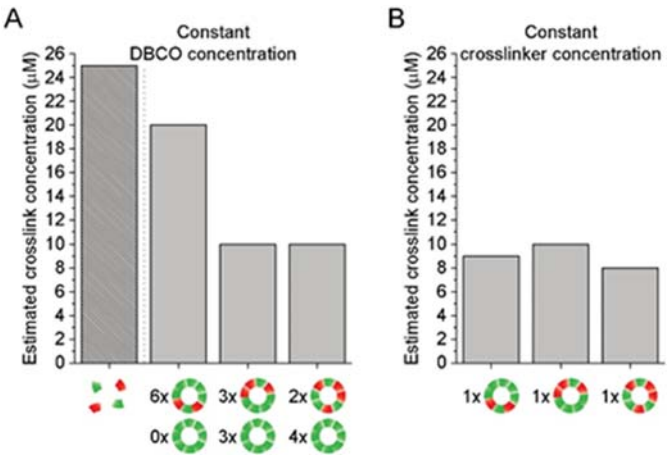

Figure 3. Estimated crosslink concentration of PIC gels, crosslinked with different amounts of CCMV capsids with different functionalization degrees. (A) Comparison of three gels, in which the total DBCO and capsid concentrations were kept constant, while varying the amount of DBCO-modified capsids (crosslinkers). As a reference, the estimated crosslink concentration of dimer-crosslinked gels is shown left. (B) Comparison of three gels, in which the amount of DBCO-modified capsids (crosslinkers) and total capsid concentration were kept constant, while varying the degree of DBCO functionalisation.

fibrin and collagen show the same behaviour.[5, 48] In these gels and also in our PIC gels, the network architecture does not change on deformation. Rather, the semi-flexible nature of the bundles or fibrils give rise to the stiffening, which –in the absence of architectural changes– is instantaneous and completely reversible. Very recently, some flexible composite gels with complex architectures have been demonstrated to also display strain-stiffening, although the exact stiffening mechanisms of these systems remain unclear.[49, 50]

An alternative mechanism to obtain stiffer gels during or after deformation are gels that change their composition or architecture when the sample is strained.[51-53] In contrast to the aforementioned mechanism, this type of strain-stiffening is slower and far from reversible. The PIC gels are intrinsically strain-stiffening, but when crosslinked with self-assembled virus-capsids, we also find the second mechanism in our material.

In semi-flexible networks at high deformation, the storage modulus is no longer a constant and it is more accurate to describe the mechanical properties by the differential modulus, $K' = \partial\sigma/\partial\gamma$ (where σ is the applied stress and γ is the resulting strain) is used to describe the mechanical behaviour of the material. At low stresses $K' = G'$, but at stresses beyond a critical value σ_c, the differential modulus becomes stress-dependent: $K' \propto \sigma^m$, where m is the stiffening index, a measure for the magnitude of the stiffening response. Rheology measurements of the capsid-crosslinked gels (at pH 5) revealed that the crosslinked PIC gels, indeed, show strain-stiffening behaviour above the same critical stress value, analogous to the non-functionalised PIC hydrogel. Additionally, for both the non-functionalised and crosslinked gel, the same stiffening index m = 1.4 (Figure 4A). At high stresses, the non-crosslinked gel **1** (orange data) fractures at applied stresses between 100 and 200 Pa. Gels containing a small molecule crosslinker, DBCO-PEG$_4$-DBCO, are more stable towards stress and continue to stiffen (light blue data).[41] Interestingly, the capsid-crosslinked gel shows a plateau in K' between σ = 140 and 200 Pa (purple data). Between samples, the plateau is reproducible, but shifts between higher or lower stresses between 100 and 200 Pa. Such plateau is also observed for fibrin hydrogels, where it is attributed to breaking of the crosslinks within the protein bundles.[4, 5] Fibrin is unique in this aspect; to the best of our knowledge, no other biological or synthetic material features this behaviour. The presence of the plateau in the crosslinked PIC gels suggests that as the stress keeps on increasing the energy is dissipated in another way in the hydrogel. We hypothesise that this observed energy dissipation is linked to the irreversible disassembly or rupture of the CCMV capsids at high stresses.

For additional support for capsid rupture, we subjected the capsid-crosslinked hydrogel to a mechanical deformation programme. In the first step, the stress was gradually increased to before (green date) or beyond (red data) the plateau stress. Subsequently, the stress was released step-wise whilst measuring K' (Figure S2). The plateau was not observed in this case, which indicates that the network changes indeed are permanent. Next, the gel was re-subjected to a gradual stress increasing. Now the plateau at ~150 Pa disappeared, but at much higher applied stress, σ = 450 Pa, a new plateau was found, which suggests that the remaining capsids, capsid fragments, and dimers rearranged and can dissipate stress once again.

Subsequent experiments were aimed at further unravelling the effect of high and low stress on the crosslinked network. In short, two samples are compared where one is deformed below the plateau stress (to σ = 120 Pa, green arrow Figure 4A) and one is deformed above the plateau stress (to 320 Pa, red arrow Figure 4A). In one approach, the sample was kept in the gel phase, where the mobility of the polymer chains is low, which will prevent significant crosslinking reactions. In a second approach, we cool the gel after deformation and measure the mechanical properties at 5 °C, where loose end of the polymer can disassemble and participate in the crosslinking process. In the

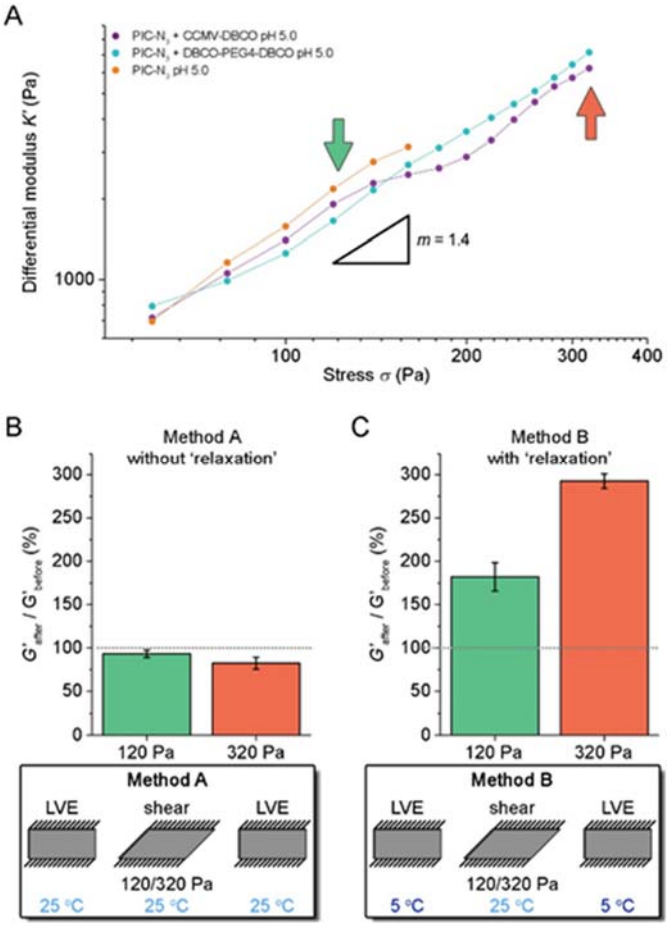

Figure 4. (A) Differential modulus K' as a function of stress σ for crosslinked PIC gels ([**1**] = 2 mg mL^{-1}) in the nonlinear viscoelastic regime. DBCO-functionalised capsid crosslinkers (purple data) are compared to a short DBCO-PEG$_4$-DBCO crosslinker (light blue data). As a control, the behaviour of the PIC gel without crosslinker was measured (orange data). The stiffening index was calculated by fitting the experimental data to a power law. (B) Recovery of the storage modulus G' after applying stresses σ just below (120 Pa) or above (320 Pa) the observed plateau (see Figure A) for DBCO-functionalised CCMV capsid crosslinkers, at T = 25 °C. (C) Recovery of G' at 5 °C, i.e. after allowing for healing through re-crosslinking. LVE = linear viscoelastic regime. The error bars represent the standard deviation of two or more measurements.

third approach, where we aimed to deform the sample at 5 °C, the gel was too soft to withstand 100 Pa stress and the sample broke prematurely. Note that the temperature programme has no effect on the PIC network itself (Supplementary Table S1).

The results of the first approach (method A) are shown in Figure 4B. The samples were subjected to stresses just below (σ = 120 Pa) or above (σ = 320 Pa) the plateau. After the stress was removed, the storage modulus G' in the linear viscoelastic (LVE) regime (γ = 4 %) of the gel was measured and compared to the initial stiffness before the stress was applied (Figure 4B). At T = 25 °C, gels that were subjected to a stress of σ = 120 Pa fully regained their original stiffness. Gels stressed above the plateau showed a small decrease in stiffness after the mechanical programme. Rupture of the capsids results in permanent network changes, which even at 25 °C, i.e. above the LCST result in a small decrease in the mechanical properties.

When the capsids are pulled apart, smaller subunits are formed (down to dimers), which will still have unreacted and accessible DBCO groups available that can participate in a subsequent crosslinking reaction as soon as they have the mobility to find a free azide. Cooling the gel below the LCST will provide such mobility and is expected to yield additional crosslinks at the damaged site, thereby improving the mechanical properties of the entire material. To confirm this assumption, the gel was subjected to stress beyond the plateau stress (to σ = 320 Pa) and the stress was released again. Then the gel was cooled to 5 °C, allowing re-crosslinking. Remarkably, the modulus of the cooled gel after deformation was over three times that of the gel before deformation (Figure 4C), strongly supporting the suggested healing mechanism. A gel stressed to σ = 120 Pa shows a similar effect, but much less pronounced.

Conclusions

We have described a new supramolecular crosslinking strategy towards biomimetic hydrogels, using protein-based viral capsids as hierarchical crosslinks. Similar to the strong natural fibrin gels, energy dissipation was observed in the strain-stiffening regime, which is probably caused by (partial) disassembly of the capsid crosslinks. This disassembly results in a higher crosslink density, increasing the storage modulus of the material. Additionally, the mechanical properties of the crosslinked gel could be tuned by changing the crosslinking temperature, and the functionalisation degree and the concentration of the crosslinker. These findings may lay the foundation for the application of these types of biomimetic hydrogels, e.g. as stress sensors or drug delivery vehicles. Further studies in this direction are aimed at investigating the release of cargo, such as a model drug or a fluorescent read-out system, from the interior of the capsids upon the application of high stresses to the crosslinked gel.

Conflicts of interest

The authors declare no conflicts of interest.

Acknowledgements

Ms. S. Rocha is acknowledged for the analysis of the crosslinked gels. All authors thank the Ministry of Education, Culture and Science (NWO Gravitation program 024.001.035) for financial support. R. J. M. Nolte acknowledges financial support from the European Research Council (ERC Advanced Grant, 740295 ENCOPOL).

Notes and references

§ Both authors contributed equally to this work.

1. R. D. Kamm and M. R. K. Wofrad, in *Cytoskeletal Mechanics: Models and Measurements*, Cambridge Univ. Press, 2006, ch. 1.
2. C. Storm, J. J. Pastore, F. C. MacKintosh, T. C. Lubensky and P. A. Janmey, *Nature*, 2005, **435**, 191-194.
3. C. P. Broedersz, K. E. Kasza, L. M. Jawerth, S. Münster, D. A. Weitz and F. C. MacKintosh, *Soft Matter*, 2010, **6**, 4120.
4. I. K. Piechocka, R. G. Bacabac, M. Potters, F. C. MacKintosh and G. H. Koenderink, *Biophys. J.*, 2010, **98**, 2281-2289.
5. I. K. Piechocka, K. A. Jansen, C. P. Broedersz, N. A. Kurniawan, F. C. MacKintosh and G. H. Koenderink, *Soft Matter*, 2016, **12**, 2145-2156.
6. N. Yamaguchi and K. L. Kiick, *Biomacromolecules*, 2005, **6**, 1921-1930.
7. N. A. Peppas, J. Z. Hilt, A. Khademhosseini and R. Langer, *Adv. Mater.*, 2006, **18**, 1345-1360.
8. Q. Wen and P. A. Janmey, *Exp. Cell Res.*, 2013, **319**, 2481-2489.
9. D. A. Gyles, L. D. Castro, J. O. C. Silva and R. M. Ribeiro-Costa, *Eur. Polym. J.*, 2017, **88**, 373-392.
10. B. V. Slaughter, S. S. Khurshid, O. Z. Fisher, A. Khademhosseini and N. A. Peppas, *Adv. Mater.*, 2009, **21**, 3307-3329.
11. J.-Y. Sun, X. Zhao, W. R. K. Illeperuma, O. Chaudhuri, K. H. Oh, D. J. Mooney, J. J. Vlassak and Z. Suo, *Nature*, 2012, **489**, 133-136.
12. Y. S. Zhang and A. Khademhosseini, *Science*, 2017, **356**.
13. E. S. Place, N. D. Evans and M. M. Stevens, *Nat. Mater.*, 2009, **8**, 457-470.
14. M. Koepf, H. J. Kitto, E. Schwartz, P. H. J. Kouwer, R. J. M. Nolte and A. E. Rowan, *Eur. Polym. J.*, 2013, **49**, 1510-1522.
15. P. H. J. Kouwer, M. Koepf, V. A. A. Le Sage, M. Jaspers, A. M. van Buul, Z. H. Eksteen-Akeroyd, T. Woltinge, E. Schwartz, H. J. Kitto, R. Hoogenboom, S. J. Picken, R. J. M. Nolte, E. Mendes and A. E. Rowan, *Nature*, 2013, **493**, 651-655.
16. M. Jaspers, M. Dennison, M. F. J. Mabesoone, F. C. MacKintosh, A. E. Rowan and P. H. J. Kouwer, *Nat. Commun.*, 2014, **5**, 5808.
17. M. Jaspers, A. E. Rowan and P. H. J. Kouwer, *Adv. Funct. Mater.*, 2015, **25**, 6503-6510.
18. R. K. Das, V. Gocheva, R. Hammink, O. F. Zouani and A. E. Rowan, *Nat. Mater.*, 2016, **15**, 318-325.

19. R. Hammink, S. Mandal, L. J. Eggermont, M. Nooteboom, P. H. G. M. Willems, J. Tel, A. E. Rowan, C. G. Figdor and K. G. Blank, *ACS Omega*, 2017, **2**, 937-945.
20. S. Mandal, Z. H. Eksteen-Akeroyd, M. J. Jacobs, R. Hammink, M. Koepf, A. J. A. Lambeck, J. C. M. van Hest, C. J. Wilson, K. Blank, C. G. Figdor and A. E. Rowan, *Chem. Sci.*, 2013, **4**, 4168-4174.
21. M. Jaspers, M. Dennison, M. F. J. Mabesoone, F. C. MacKintosh, A. E. Rowan and P. H. J. Kouwer, *Nat. Commun.*, 2014, **5**.
22. J. P. Gong, *Soft Matter*, 2010, **6**, 2583-2590.
23. M. A. Haque, T. Kurokawa and J. P. Gong, *Polymer*, 2012, **53**, 1805-1822.
24. M. Jaspers, S. L. Vaessen, P. van Schayik, D. Voerman, A. E. Rowan and P. H. J. Kouwer, *Nat. Commun.*, 2017, **8**, 15478.
25. J. Li, W. R. K. Illeperuma, Z. Suo and J. J. Vlassak, *ACS Macro Lett.*, 2014, **3**, 520-523.
26. M. Goldberg, R. Langer and X. Q. Jia, *J. Biomater. Sci. Polym. Ed.*, 2007, **18**, 241-268.
27. Q. Wang, J. L. Mynar, M. Yoshida, E. Lee, M. Lee, K. Okuro, K. Kinbara and T. Aida, *Nature*, 2010, **463**, 339-343.
28. J. Luckanagul, L. A. Lee, Q. L. Nguyen, P. Sitasuwan, X. Yang, T. Shazly and Q. Wang, *Biomacromolecules*, 2012, **13**, 3949-3958.
29. J. A. Luckanagul, L. A. Lee, S. You, X. Yang and Q. Wang, *J. Biomed. Mater. Res. A*, 2015, **103**, 887-895.
30. H. Wang and S. C. Heilshorn, *Adv. Mater.*, 2015, **27**, 3717-3736.
31. S. R. Deshpande, R. Hammink, R. K. Das, F. H. T. Nelissen, K. G. Blank, A. E. Rowan and H. A. Heus, *Adv. Funct. Mater.*, 2016, **26**, 9075-9082.
32. S. R. Deshpande, R. Hammink, F. H. T. Nelissen, A. E. Rowan and H. A. Heus, *Biomacromolecules*, 2017, **18**, 3310-3317.
33. S. Nagahara and T. Matsuda, *Polym. Gels Networks*, 1996, **4**, 111-127.
34. J. A. Speir, S. Munshi, G. Wang, T. S. Baker and J. E. Johnson, *Structure*, 1995, **3**, 63-78.
35. D. L. Caspar and A. Klug, *Cold Spring Harbor Symp. Quant. Biol.*, 1962, **27**, 1-24.
36. A. Zlotnick, R. Aldrich, J. M. Johnson, P. Ceres and M. J. Young, *Virology*, 2000, **277**, 450-456.
37. M. Comellas-Aragonès, H. Engelkamp, V. I. Claessen, N. A. J. M. Sommerdijk, A. E. Rowan, P. C. M. Christianen, J. C. Maan, B. J. M. Verduin, J. J. L. M. Cornelissen and R. J. M. Nolte, *Nat. Nanotechnol.*, 2007, **2**, 635.
38. A. Liu, M. Verwegen, M. V. de Ruiter, S. J. Maassen, C. H. H. Traulsen and J. J. L. M. Cornelissen, *J. Phys. Chem. B*, 2016, **120**, 6352-6357.
39. M. A. Kostiainen, P. Hiekkataipale, A. Laiho, V. Lemieux, J. Seitsonen, J. Ruokolainen and P. Ceci, *Nat. Nanotechnol.*, 2013, **8**, 52-56.
40. M. A. Kostiainen, O. Kasyutich, J. J. L. M. Cornelissen and R. J. M. Nolte, *Nat. Chem.*, 2010, **2**, 394-399.
41. D. C. Schoenmakers, A. E. Rowan and P. H. J. Kouwer, 2017, Under consideration at *Nat. Commun.*
42. C. A. Hommersom, B. Matt, A. van der Ham, J. J. Cornelissen and N. Katsonis, *Org. Biomol. Chem.*, 2014, **12**, 4065-4069.
43. N. F. Steinmetz, V. Hong, E. D. Spoerke, P. Lu, K. Breitenkamp, M. G. Finn and M. Manchester, *J. Am. Chem. Soc.*, 2009, **131**, 17093-17095.
44. P. H. J. Kouwer, P. de Almeida, O. ven den Boomen, Z. H. Eksteen-Akeroyd, R. Hammink, M. Jaspers, S. Kragt, M. F. J. Mabesoone, R. J. M. Nolte, A. E. Rowan, M. G. T. A. Rutten, V. A. A. Le Sage, D. C. Schoenmakers, C. Xing and J. Xu, *Chin. Chem. Lett.*, 2017, **28**, DOI: 10.1016/j.cclet.2017.1011.1002.
45. E. Gillitzer, D. Willits, M. Young and T. Douglas, *Chem. Commun.*, 2002, 2390-2391.
46. J. M. Eeftens, J. van der Torre, D. R. Burnham and C. Dekker, *BMC Biophysics*, 2015, **8**, 9.
47. M. L. Gardel, J. H. Shin, F. C. MacKintosh, L. Mahadevan, P. Matsudaira and D. A. Weitz, *Science*, 2004, **304**, 1301-1305.
48. F. C. MacKintosh, J. Käs and P. A. Janmey, *Phys. Rev. Lett.*, 1995, **75**, 4425-4428.
49. G. K. Tummala, T. Joffre, R. Rojas, C. Persson and A. Mihranyan, *Soft Matter*, 2017, **13**, 3936-3945.
50. B. Yan, J. Huang, L. Han, L. Gong, L. Li, J. N. Israelachvili and H. Zeng, *ACS Nano*, 2017, **11**, 11074-11081.
51. Z. Oztoprak and O. Okay, *Int. J. Biol. Macromol.*, 2017, **95**, 24-31.
52. X. Zhang, C. Zhao, N. Xiang and W. Li, *Macromol. Chem. Phys.*, 2016, **217**, 2139-2144.
53. Y. H. Tran, M. J. Rasmuson, T. Emrick, J. Klier and S. R. Peyton, *Soft Matter*, 2017, **13**, 9007-9014.